Development 140, 2848 (2013) doi:10.1242/dev.098921

A high-throughput template for optimizing *Drosophila* organ culture with response-surface methods

Jeremiah Zartman, Simon Restrepo and Konrad Basler

There were two errors published in *Development* **140**, 667-674.

The insulin value for WM1 was incorrectly stated in the text on p. 671. The true value is 6.2 μg/ml, not 3.1 μg/ml as stated in the text, and the insulin concentration in supplementary material Table S1 should read 0.005 mg/ml.

The authors apologise to the readers for these errors.

Development 140, 667-674 (2013) doi:10.1242/dev.088872

A high-throughput template for optimizing *Drosophila* organ culture with response-surface methods

Jeremiah Zartman*,‡, Simon Restrepo* and Konrad Basler§

SUMMARY

The *Drosophila* wing imaginal disc is a key model organ for molecular developmental genetics. Wing disc studies are generally restricted to end-point analyses of fixed tissues. Recently several studies have relied on limited data from discs cultured in uncharacterized conditions. Systematic efforts towards developing *Drosophila* organ culture techniques are becoming crucial for further progress. Here, we have designed a multi-tiered, high-throughput pipeline that employs design-of-experiment methods to design a culture medium for wing discs. The resulting formula sustains high levels of proliferation for more than 12 hours. This approach results in a statistical model of proliferation as a function of extrinsic growth supplements and identifies synergies that improve insulin-stimulated growth. A more dynamic view of organogenesis emerges from the optimized culture system that highlights important facets of growth: spatiotemporal clustering of cell divisions and cell junction rearrangements. The same approach could be used to improve culture conditions for other organ systems.

KEY WORDS: Cl.8, Cell culture media development, Growth, Imaginal, Proliferation, Wing disc

INTRODUCTION

The growth and development of the *Drosophila* wing imaginal disc has served as a 'flagship' model organ for a diverse range of studies on morphogen activity, pattern formation, growth control, epithelial cell-cell interactions, pattern formation and compartment boundary formation (Affolter and Basler, 2007; Crick and Lawrence, 1975; De Celis, 2003; Eaton, 2003; Neto-Silva et al., 2009; Schwank et al., 2011). Wing disc development lasts ~96 hours, during which the disc grows from 50 to 50,000 cells (Fain and Stevens, 1982; Garcia-Bellido and Merriam, 1971). The wing disc is geometrically simple, consisting of two epithelial layers that become folded in a stereotypic pattern during development (Ashburner et al., 2005; Ursprung et al., 1972).

Progress in *Drosophila* genetics continues to permit ever-higher degrees of sophisticated analyses of many developmental processes that are difficult to study in other systems (Belacortu and Paricio, 2011; Bischof et al., 2007; Elliott and Brand, 2008; Pearson et al., 2009; Yagi et al., 2010). However, the majority of studies to date have relied on measuring properties from populations of fixed, immunostained tissues owing to the difficulty of immobilizing and imaging living larvae and the lack of *in vitro* methods that recapitulate wing disc growth and development.

Pioneering studies on the primary culture of wing discs and wing disc derived cells by Wyss, Milner, Robb and Miyake in the late 1960s until the 1980s described different medium compositions that allowed for the transient *in vitro* maintenance of wing discs fragments (Robb, 1969; Wyss, 1982) and the establishment of stable disc-derived cell lines (Currie et al., 1988; Ui et al., 1987). Recently, several studies have employed short-term culture and live imaging of wing discs (Aldaz et al., 2010; Gibson et al., 2006; Kicheva et al., 2007; Landsberg et al., 2009; Mao et al., 2011; Ohsawa et al., 2012). However, there have been no recent reported efforts to develop media specifically for *Drosophila* organ culture, perhaps owing to the inherent difficulty involved in such a project. In this study, we decided to follow a multidisciplinary approach towards developing a culture medium that supports high levels of proliferation in freshly explanted discs by applying mathematical tools such as design-of-experiments and response-surface methodology to accelerate the exploration of the experimental parameter space and to account for multifactorial interactions (Mandenius and Brundin, 2008).

To overcome a bottleneck in the number of dissected wing discs that could be prepared to test multiple media formulae, we hypothesized that a cell line that was derived from wing imaginal discs called Clone.8 (Cl.8) could be used as a proxy for wing disc proliferation (Currie et al., 1988). In the first step of the optimization pipeline, concentrations of media components were varied based on mixing experiments and response-surface methodology (RSM) where proliferation was the chosen response variable. Application of ANOVA results in a fitted polynomial model of the data. In the second stage, an optimized culture medium formula for Cl.8 proliferation was subsequently tested in a disc culture bioassay that scores the number of mitotic cells that can be observed in fixed discs after a certain culture period. Finally, a third, quality control, stage eliminated artefacts that might have arisen during the previous stages by directly monitoring cell divisions with a flexible live-imaging setup.

Our optimization pipeline enabled us to identify crucial medium components that are required to sustain cell division *in vitro* for significant periods and at high growth rates (>20% growth in under 12 hours, supplementary material Movie 1). Live-imaging studies with the improved medium provide a clear demonstration of frequently observed spatiotemporal clusters of mitotic cells, transient T1 transitions and cell rearrangements, which were not noted in previous live-imaging studies. The frequency and functional importance of patterned mitotic clustering has been a point of uncertainty and observations of cell rearrangements hint

Institute of Molecular Life Sciences, University of Zurich, Winterthurerstrasse 190, Zurich CH-8057, Switzerland.

*These authors contributed equally to this work
‡Present address: Department of Chemical and Biomolecular Engineering, University of Notre Dame, 182 Fitzpatrick Hall, Notre Dame, IN 46556, USA
§Author for correspondence (konrad.basler@imls.uzh.ch)

Accepted 12 November 2012

that the tissue is more dynamic than previously thought (Adler and MacQueen, 1981; Aegerter-Wilmsen et al., 2010; Milán et al., 1996). Our work allows the study of growing wing discs *in vitro* and provides a pipeline to further improve culture conditions in an effort to recapitulate wing disc development *in vitro*. Finally, the medium development pipeline presented here can be modified to optimize other model organ systems efficiently and rationally, given severe technical constraints of acquiring the large numbers of organs needed for high-throughput assays that cover a large experimental parameter space.

MATERIALS AND METHODS

Cell culture

Cl.8 cells were maintained in the M3-based reference medium, M3RM medium (elsewhere called Cl.8 medium), which contains both inactivated mammalian serum and fly extract (Fig. 1A; supplementary material Table S1) in an incubator at 25°C. For maintenance, cells were passaged at a 1:3 or 1:4 dilution every 3-4 days in T25 plates (Corning). The cell growth

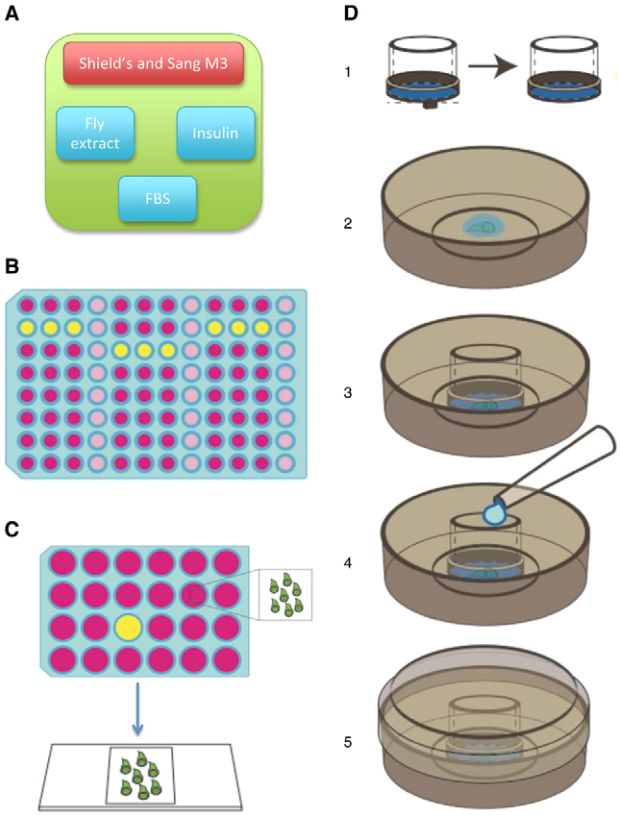

Fig. 1. Optimization strategy for imaginal cell culture media development. (**A**) The composition of M3RM, the medium supporting Cl.8 growth. (**B**) High-throughput screen using Cl.8 cells as a proxy for disc growth. Each medium formulation was tested in three separate wells to provide technical replicates. A fourth blank well was used to estimate the background signal. (**C**) Proliferation assay for wing discs. Multiple wing discs were cultured in 24-well plates with 400 µl of medium and then fixed briefly with paraformaldehyde and mounted for imaging. (**D**) Live imaging setup. (1) A culture chamber was devised for live imaging that uses porous filters to provide oxygenation and backpressure to prevent significant motion of the disc during live imaging. (2) About 10 µl of media containing carefully dissected discs are placed on a glass bottom dish. (3) The filter is placed on top of the drop of medium. (4) Additional medium (~100 µl) is added. (5) The chamber is sealed with parafilm after lining the chamber PBS-soaked filter paper to provide a humid environment.

assays were initiated with 40,000 cells per well (1.18×10^5 cells/cm^2) in 96-well plates (Greiner Bio-one Cellstar) in 100 µl of culture medium and incubated for 4 days. Each independent experiment was performed in triplicate (three wells) with random assignment of culture conditions with a fourth well containing medium as a blank. Fetal bovine serum (AG biochrom) was heat-inactivated at 56°C for 30 minutes. Fly extract was prepared from *yw* flies according to the recipe of Milner and colleagues (Currie et al., 1988).

Disc culture

Staged 4-day-old larvae (96-100 hours after egg deposition) were washed once with 70% ethanol and twice with PBS. Wing discs were dissected in a horizontal flow hood directly in culture medium drops on siliconized glass (Sigmacote, Sigma). Care was taken to not rupture the gut during dissection in order to preserve sterility. Dissected discs were transferred to non-adhesive 24-well (Hydrocell, Nunc) plates with a micropipette. Non-adhesive wells proved to be slightly beneficial for long-term culture compared with traditional tissue culture-treated wells. The disc cultures were stored either in a 25°C incubator or in a Styrofoam box at room temperature (22°C).

Bioassay for wing disc cell proliferation

Wing disc cells dramatically expand their apical area during M-phase, enabling rapid visual detection of dividing cells with a YFP-expressing septate junction marker (LAC::YFP) (Kyoto Stock Center). For wing disc proliferation experiments, the number of large, M-phase cells was counted from *z*-stack confocal images within a quadrat focused on the wing pouch after a given period of culture followed by fixation with paraformaldehyde solution. Investigation of the dynamics of cell division on the apical surface relies on a line with GFP inserted into the E-Cadherin locus (Huang et al., 2009). The quadrat was defined as 135 µm^2, corresponding to the field of view available on the Zeiss 710 with a 63× oil microscope set to a digital zoom of one. For 3rd instar wing discs (96-120 hour AEL), the number of total counted mitoses observed in discs that are fixed immediately is relatively independent of disc size. For example, for staged discs at 96 hours AEL, we observed 32±13 mitoses/quadrat (n=19); for staged discs at t=120 hour, we counted 36±12 mitoses/quadrat (n=38). Thus, the bioassay is relatively robust to variations in disc size.

Live imaging

Approximately 10 µl of the growth medium containing 1-2 wing discs was transferred by a 20 µl pipette to an uncoated glass bottom dish with a 20 mm diameter glass bottom (Mattek). The disc was positioned with a tungsten needle with the peripodial membrane facing downwards. Next, a Millicell polycarbonate cell culture insert (8.0 µm pore, Millipore #PI8P01250) was placed on top of the culture drop after clipping the feet (which leaves ~60 µm gap between the plastic rim and the filter). Filter paper dampened with PBS surrounded the rim of the glass bottom dish and the lid was sealed with parafilm. Both a single-point laser confocal microscope (Zeiss 710) and a spinning-disc confocal microscope (Andor) were used for obtaining time-lapse images with the spinning-disc confocal providing superior results during long-term live-imaging experiments, probably owing to reduced phototoxicity.

Reagents

The sources and concentrations of the reference serum-containing medium are listed in supplementary material Table S1. Other reagents include: Schneider's *Drosophila* Medium 1× (Invitrogen, #21720, lot numbers are listed in the text), IPL41 (Invitrogen, #11403), Sf900 II SFM (Invitrogen, #10902), TC-100 (Invitrogen, #13055) and D22 (US Biological, #D9600).

Cell proliferation assay

Unless otherwise indicated, cell counts were estimated using the CyQUANT Direct Cell Proliferation Assay Kit (Invitrogen). Fluorescence measurements were acquired with a plate reader (Promega Glomax MultiDetection system). Cl.8 cells are semi-adherent cells, do not show contact inhibition and continue to grow as clusters after reaching confluency. To provide a more uniform signal, cells were manually resuspended before the fluorescence reading and then spun down for 1

minute at 470 ***g*** to remove air bubbles. Background intensity blanks were subtracted from raw intensity readings of each of the triplicate conditions. A calibration curve showed a linear relationship between background subtracted fluorescent intensity readings and known cell numbers counted from a hemocytometer (supplementary material Fig. S1).

Experimental design and statistical analysis

Experimental design and data analysis were performed using Design-Expert software (version 8.0.5, Stat-Ease, MN, USA).

RESULTS

High-throughput optimization of a wing disc culture medium using Cl.8 cells as a proxy

Improving culture conditions for wing discs requires developing high throughput methods to quantify how the medium composition affects disc vitality and growth. Execution of such a systematic analysis of nutritional requirements with explanted wing discs is hindered by the bottleneck posed by the delicate manual dissection step (~2-3 minutes/larvae for an experienced operator attempting sterile dissection) and the lack of a sensitive quantitative assay measuring either wing disc health or proliferation. Thus, the development of a high-throughput optimization pipeline became the first challenge in improving the reference culture medium (Fig. 1).

To overcome the dissection bottleneck, we chose to use the Cl.8 cell line as a high-throughput amenable proxy for wing discs and the Cl.8 maintenance medium as the starting medium composition (here called M3RM) (Fig. 1A,B; supplementary material Table S1). Cl.8 cells were derived close to 30 years ago and their physiological requirements could have drifted significantly from primary disc cells. However, a recent report by modENCODE suggests that Cl.8 cells maintain a transcriptional profile similar to that of cells near the intersection of the A/P and D/V boundaries in the wing disc (Cherbas et al., 2011). Cl.8 cells have been shown to be very sensitive to exogenous growth factors and, in addition to fetal bovine serum (FBS) and insulin, also require a fly extract that contains heat-stable proteins. For example, previous studies on Cl.8 cells were instrumental in identifying the family of imaginal disc growth factors and adenosine deaminase-related growth factors (Kawamura et al., 1999; Zurovec et al., 2002). Although other wing disc cell lines exist and are now available, Cl.8 cells historically have been the most frequently employed in biochemical studies, including in our lab, and this availability resulted in the initial selection of Cl.8 cells. Pilot experiments further supported our decision to use Cl.8 cells as a proxy for wing disc growth.

Additional efficiency in exploring the parameter space was achieved with multifactorial screens based on design-of-experiments methodology, an approach frequently used in the optimization of processes (Jeon et al., 2010). Multifactorial screens can provide efficient identification of key medium components. In this study, we looked at varying the composition of basal medium by mixing commercially available media in different proportions while keeping the other components constant, including insulin, fly extract (FEX) and fetal bovine serum (FBS). Based on these results, we then employed a further round of response-surface methods (RSM), which provide a statistical model of Cl.8 proliferation as a function of the best basal medium and concentrations of growth supplements. The optimal composition for Cl.8 cells was then tested on wing disc cultures. For this step, we developed a proliferation bioassay to compare different pools of explanted wing discs (see Materials and methods). Finally, we developed a live-imaging method that enables observation of cell proliferation over an extended period of time and can easily enable media exchange for long-term culture experiments (Fig. 1D).

Identification of the best commercially available basal medium for wing disc culture

First, we performed a blending screen of six different basal media for insect cell culture, while keeping the supplements (FBS, FEX and insulin) at the reference concentrations in M3RM (supplementary material Table S1). Of the media tested, M3, Schneider's and D22 are frequently used for the maintenance of *Drosophila* lines (Echalier, 1997). IPL-41, TC-100 and Sf900 II have been successfully used in the cultivation of *Drosophila* S2 cells (Batista et al., 2008; Bovo et al., 2008). The media-blending experiment was designed as an efficient method to search the parameter space of concentrations of essential nutrients such as amino acids, salts, sugars and vitamins by varying the relative proportions of the basal media in the culture medium mixture.

A simplex centroid design for fitting a quadratic model was used resulting in 96 runs with a total of four blocks (each block was a 96-well plate) (Scheffe, 1963). The simplex centroid design includes the vertices (each of the undiluted basal media), the center points of the edges (50:50 mixes of two different basal media), as well as triple blends (three basal media in proportions of 1/3, 1/3, 1/3) and the overall centroid (all six media in equal proportions). Summaries of the experimental design, ANOVA analysis and model coefficients are presented in supplementary material Tables S3-S5 and notes on the data analysis are provided in Appendix S1.

Surprisingly, Schneider's medium, which is not routinely used to culture Cl.8 cells, performed much better than any of the other basal media (including M3) or any blend without requiring any type of adaptation (Fig. 2A,B, ~60% higher density). All blends containing Schneider's medium showed a dilution effect in relation to the amount of Schneider's medium in the blend, and both D22 and Sf-900 II were toxic for Cl.8 cells.

Schneider's medium enhances the proliferative response of Cl.8 cells to insulin

One explanation for the difference in Cl.8 proliferation between Schneider's and M3-based formulations could be changes in the synergistic effects of supplements in the different basal media. Preliminary experiments in our lab showed that FEX was crucial to growth in M3 medium but that insulin was surprisingly dispensable (data not shown). To quantitate the effects more clearly, we employed response-surface methods (RSMs) to produce topological maps of proliferation as a function of supplements for both M3 and Schneider's basal media. An IV-optimal design distributed over three blocks served as the final design in which the basal media were treated as categorical variables (design points shown in Fig. 2C,D). The concentration of each supplement ranges from complete absence to twice the concentration of the standard supplement concentration (supplementary material Table S6). Experimental details and data analysis notes are provided in supplementary material Appendix S1 and Tables S7-S9.

Graphically exploring the response-surface model parameter space provided several insights (Fig. 2E-H). Notably, Cl.8 cells proliferated more in Schneider's than in M3 media only when insulin was added to Schneider's medium (Fig. 2H). These results imply that Cl.8 cells had not lost the inherent ability to respond to insulin, but rather that the response of insulin depends on the composition of the basal medium.

Furthermore, higher levels of FEX appeared to partially replace the need for FBS as a growth supplement (Fig. 2G; supplementary

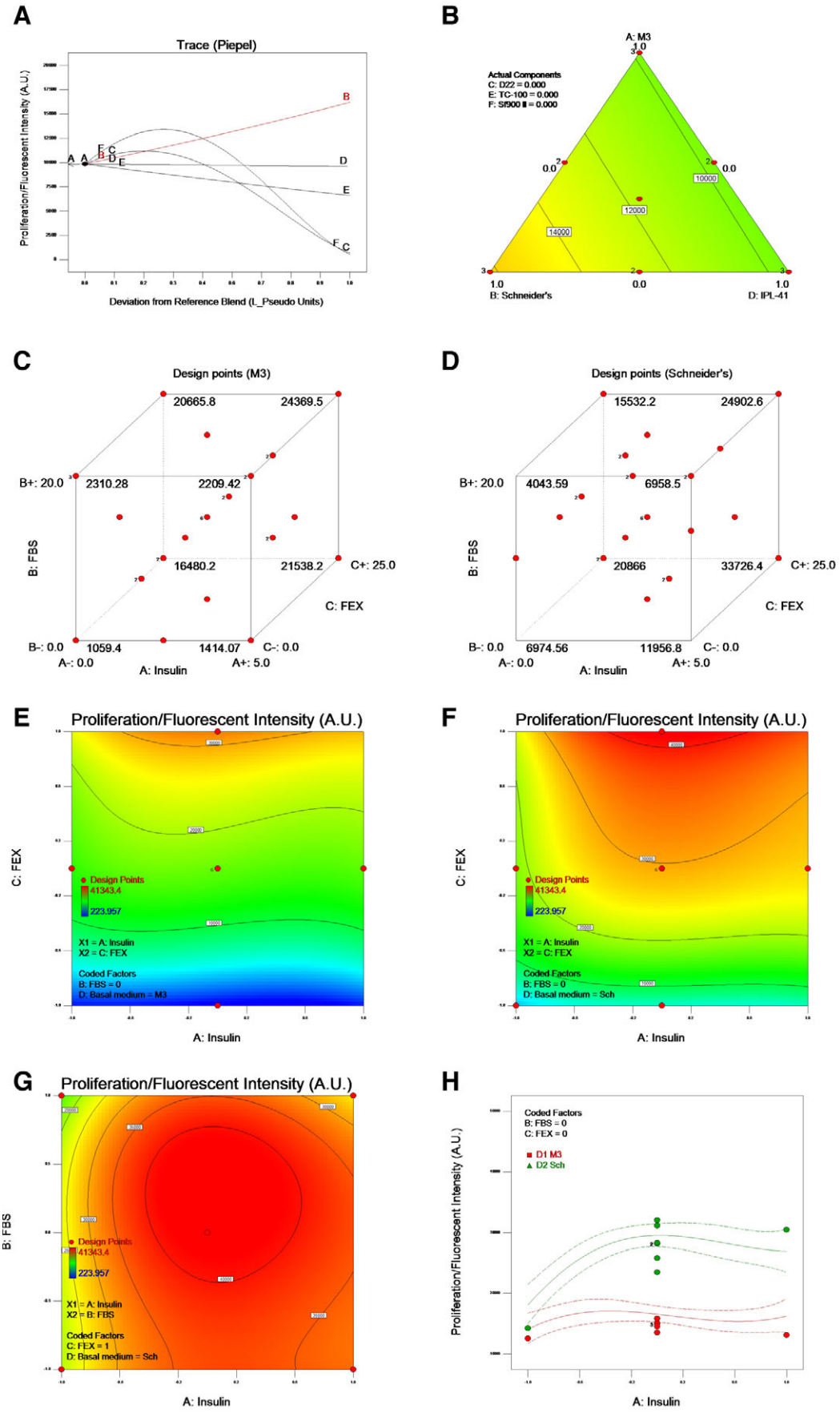

Fig. 2. See next page for legend.

Fig. 2. Optimization of Cl.8 cell proliferation. (**A**) The blending experiment included six components (basal media, which are listed in supplementary material Table S2). The design points and response values are listed in supplementary material Table S3. Trace plot showing the change in proliferation as the reference blend (~100% M3) is systematically varied to include other basal media. Schneider's (listed as medium B on the plot) permitted more cell growth than the basal medium used (M3, marked as medium A on the plot). Proliferation is in arbitrary units of fluorescence from the CyQUANT cell proliferation assay. (**B**) Contour plot of the three best performing basal media: Schneider's, M3 and IPL-41. All other mixture components are set to 0. (**C**,**D**) Design points for the RSM experiment for each categorical variable, M3 (C) and Schneider's basal medium (D). Red points within the cuboidal space represent the design points within the coded parameter space (–1, no supplement added; +1, twice the concentration of the given supplement in M3RM; supplementary material Table S6). The numbers next to the red points represent the number of replicates at that point. (**E**,**F**) Contour plot of cell proliferation (fluorescent intensity, A.U.) as a function of FEX and insulin, with 2% FBS in either a M3 (E) or Schneider's (F) background. (**G**) Contour plot as a function of FBS and insulin, with 5% FEX (high levels) in Schneider's. The effect of adding FBS near the optimal concentrations of FEX and insulin did not appear to be strong. We thus opted to omit FBS from WM1 to represent a simpler formulation. (**H**) Interaction plot of proliferation as a function of insulin in either M3 (red) or Schneider's (green), with 2% FBS and 2.5% FEX.

material Table S9). These experiments demonstrate that response-surface methods can be an effective tool for exploring how extrinsic signals interact with each other and are useful for revealing local and global maxima within the experimental design space. Thus, by employing RSMs we were able to explain the differences in Cl.8 growth rates in Schneider's or M3-based formulations. In addition, we could use the RSM results to predict optimal culture medium formulations for the different variables that we tested.

Validating an optimized medium for *in vitro* culture of wing imaginal discs

Wing discs cultured in the reference medium (M3RM) showed a quick decline in proliferation (Fig. 3A). Based on the Cl.8 cell optimization data, we formulated a new culture medium called Wing Disc Medium 1 (WM1). The new medium eliminates the use of FBS (to rely on a single fly-based 'serum') and increases FEX to 5% with a slightly higher concentration of insulin (3.1 μg/ml) in a Schneider's medium background. WM1 more than doubled the proliferation rate of wing disc cells (compared with M3RM) after both 5 hours at 25°C and 18 hours at room temperature (~22°C) (Fig. 3B,C). Therefore, WM1 sustains cell proliferation in wing discs at rates closer to *in vivo* rates for significantly longer periods. Based on this quantifiable improvement, we are now robustly performing live-imaging assays of wing discs cultured in WM1 with high proliferative activity to examine a large range of experimental variables.

Spatiotemporal clustering of cell divisions and cell rearrangements are apparent in the improved culture protocol

To illustrate the potential of WM1, we found that the improved formula enables observations of discs showing more than 20% proliferation under high-resolution imaging conditions (one example is shown in Fig. 4A,B). Strikingly, cell divisions do not follow a random distribution; rather, cell divisions are often

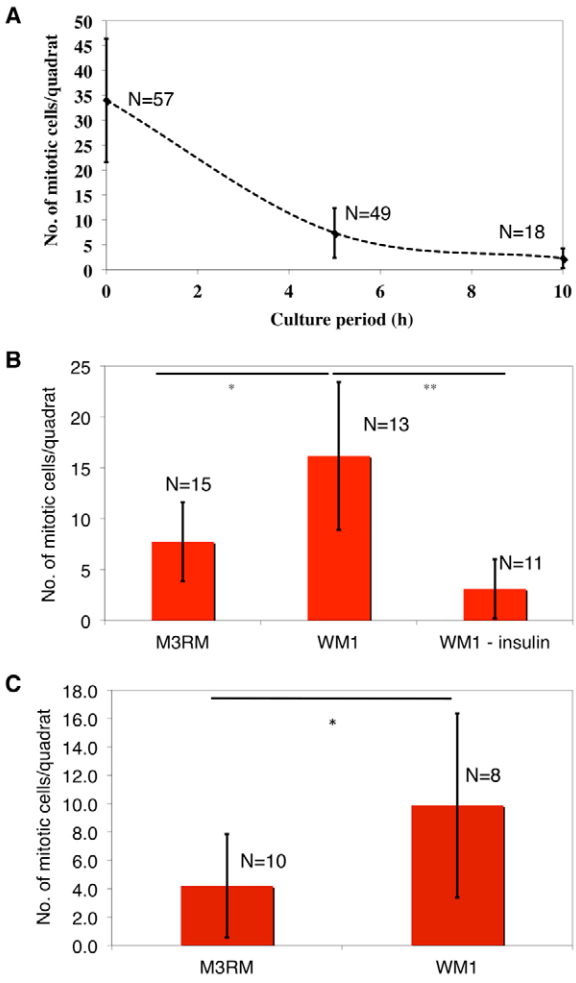

Fig. 3. Validation of optimized medium for wing disc culture. (**A**) Mitotic rate decreases in wing discs cultured in Cl.8 medium with very low rates of mitoses after 10 hours of culture at 25°C. The quadrat is defined as a 0.0182 mm^2 area centered on the D/V and A/P axes. (**B**) WM1 leads to significantly higher levels of proliferation after 5 hours of culture at 25°C. Insulin is a necessary component for proliferation (*P=8×10^{-4}, two tail t-test of the square-root transformed count data, assuming equal variance; **P=5×10^{-6}). (**C**) The mitotic rate remains more than twofold higher in the optimized medium WM1 after 18 hours of culture at room temperature (*P=0.04, two tail t-test of the square-root transformed count data, assuming equal variance). All error bars show s.d.

grouped in spatiotemporal clusters (Fig. 4A). This observation reinforces previous work by Milán et al. on spatial clustering and highlights a new level of cell division organization at the temporal level (Milán et al., 1996). Several examples of spatiotemporal clusters are presented in Fig. 4B. Here, we considered that cells were part of a cluster if they divided in sequence along a given direction. Selected clusters are color coded such that groups of direct neighbors that form a cluster share the same color. When direct neighbors divided along different directions we chose two different colors. A more-detailed quantitative analysis of mitotic clusters in the growing wing discs is the subject of another study.

As a second demonstration of the improved method, time-lapse analysis also revealed multiple instances when cell topology and polygon count frequently changed between timeframes. This counters a common assumption that there are rarely cell

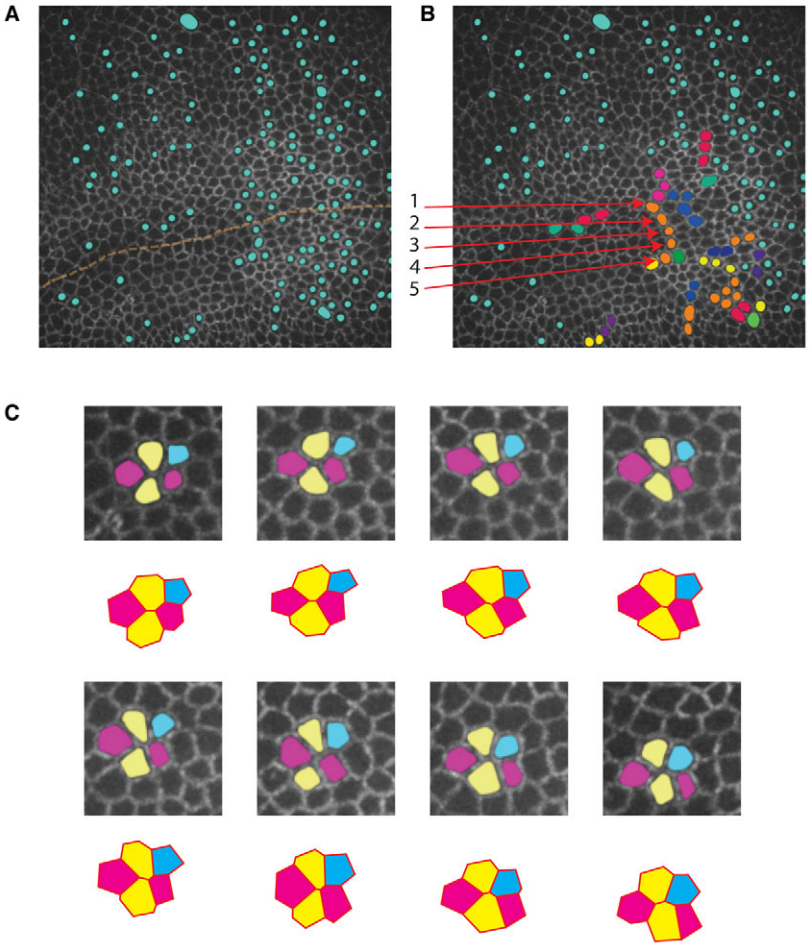

Fig. 4. Spatiotemporal clustering of cell division and cell rearrangements. (**A**) Representation of all cells that have divided (marked in blue) over a 9.5-hour time period. Many dividing cells are in direct proximity. The broken line is an estimated and approximate dorsal-ventral boundary. The long axis of many clusters is perpendicular to the DV axis, a feature previously observed based on clonal analysis. (**B**) Same time-lapse experiment as in A. Representation of groups of cells that divided in sequence both in time and in space (directionally). Not all the clusters that happened are highlighted here, just some representative examples. (**C**) An example of cell intercalation. The blue-marked cell eventually becomes a direct neighbor of the bottom yellow-marked cell. Panels show cells at 15-minute intervals.

rearrangements during wing disc growth (Gibson et al., 2006). We found that cell topology at this stage of development is very dynamic. Four edge vertices appear to be inherently unstable and often oscillate between two possible configurations through T1 transitions. We also observe that short edges are equally unstable and that in positions in which several short edges are in close proximity this can even lead to cell intercalations during the latter stages of 3rd instar discs (Fig. 4C).

DISCUSSION

Optimization of an organ culture medium

Hemolymph constitutes the external milieu of imaginal tissues and provides necessary requirements for tissue homeostasis, growth and differentiation. One of the main challenges in obtaining an optimal culture medium for wing discs stems from the largely undefined complexity of hemolymph. Basal insect cell culture media were developed partly by mimicking the major ion and amino acid composition of hemolymph. The differences between different culture media reflect the given state of knowledge on hemolymph composition and iterative experimentation. Other unknown metabolites are provided by yeast extract, FBS or FEX. This study shows that the differences in media composition can have strong effects. For example, the composition of the basal medium affects the strength of the proliferative response to insulin.

The importance of fly extract for supplementing the basal medium raises the question of what are the active factors necessary for wing disc growth *in vitro* and *in vivo*? We have confirmed by ultrafiltration that the crucial components of fly extract are of large molecular weight, most likely proteins (data not shown). Recently, ferritin was identified as a component of fly extract that stimulates Cl.8 growth (Li, 2010). We have found that mammalian ferritin can stimulate growth, but is not sufficient for replacing fly extract for long-term culture of Cl.8 cells in serum-free media (data not shown).

Importantly, nonlinear interactions between the large number of culture medium components makes identification of optimal concentrations a nontrivial ‘systems-level’ task. Our results point to the necessity of redeveloping basal media for *Drosophila* cells and organs in a fully documented, rational and quantitative manner, and in functionally characterizing the multifactorial interactions between growth factors found in hemolymph.

The role of insulin

Based on the importance of the *Drosophila* homologs of insulin to the regulation of wing size, we were surprised that insulin showed such a weak effect on Cl.8 growth. Furthermore, it seemed to contradict the earlier findings of Milner and colleagues on related cell lines (Cullen and Milner, 1991), but appeared to agree with observations of insulin by Bryant and colleagues (Kawamura et al., 1999). We initially attributed the difference to changes in the Cl.8 cell line over time (over 20 years have elapsed between the studies). However, the finding that Cl.8 cells still respond to insulin in other basal media such as Schneider’s (and IPL-41, data not shown) has added an interesting twist to the characterization of the behavior of the cell. The contextual response of Cl.8 cells to insulin highlights

the crucial influence of the basal medium composition on results obtained from *in vitro* culture. Response-surface methods were thus instrumental in identifying Cl.8 cells as a possible model to study conditional insulin resistance, and thus raises many additional questions that remain to be addressed in future studies.

Spatiotemporal clustering of cell divisions

One of the surprising observations made from live-imaging experiments of wing discs in WM1 is the extent of spatiotemporal clustering of cell divisions, a phenomenon first described by the lab of Garcia-Bellido (Milán et al., 1996). The extent to which cell divisions are clustered, and thus possibly coordinated, has remained somewhat controversial given the difficulty in interpreting clusters from fixed images (Aegerter-Wilmsen et al., 2010). In general, we find that live-imaging of discs that show higher numbers of dividing cells also frequently exhibit more prominent clustering of cell division, highlighting that these phenomena are related to how actively a disc is dividing. These clusters could have been missed in previous live-imaging studies if insufficient levels of proliferation were sustained by the medium employed. Most cells in late 3rd instar wing discs are stalled in G2 (Neufeld et al., 1998). The observed cell division clustering in the wing disc suggests that the decision to start M-phase might be regulated at some level between neighboring cells, perhaps through gap junction communication (Bryant and Fraser, 1988; Jursnich et al., 1990). Indeed, a proper appreciation of spatiotemporal clustering might be required to properly interpret some experiments that rely on clonal analysis (Griffin et al., 2009). As cell divisions are often clustered, this phenomenon might occur more frequently than expected, which will be examined in future work.

Cell junction dynamics

The observed dynamics of epithelial remodeling in 3rd instar wing discs was another unexpected surprise given the assumption in the field of low levels of cell rearrangements (Gibson et al., 2006). Sub-optimal media conditions may have prevented observation of the full dynamics of organ growth, suggesting that the forces generated by cell proliferation and growth fade away quickly, masking the extent to which rearrangements and translocations normally happen. Our results highlight that cell topology during wing disc development shows unexpected dynamics that deserve further characterization (Classen et al., 2005; Griffin et al., 2009). Therefore, our results underscore the need to consider the medium composition and performance as an important variable in live-imaging studies of wing imaginal discs.

Outlook

This study represents the first rational, multifactorial analysis of the growth requirements of *Drosophila* wing imaginal disc culture, and provides an optimization pipeline that can be adapted to improve wing disc culture techniques further. By identifying a crucial role for fly extract and an important synergy between insulin and Schneider's medium, the average permissive period for cell division of cultured wing discs is extended by more than 100% compared with the reference medium used in establishing the Cl.8 cell line. WM1 allows robust cell proliferation to take place for more than 18 hours at room temperature. This time window could be appropriate for the study of many questions of interest, such as the role of mechanical forces in wing growth development. Future improvements to WM1 will likely require the development of an optimal basal medium that improves on the capacities of Schneider's medium, the fractionation of fly extract to identify its crucial components, as well as a systems-level analysis of the adaptation of wing discs to culture conditions.

This culture method provides an efficient means to combine genetic, mechanical and pharmacological techniques for studying organ development and physiology. The strategy of identifying a proxy for the initial stages of culture optimization followed by a more limited optimization step with explanted organs might be a useful approach for other model organ systems. This method could serve as a starting point for the future development of culture techniques, allowing the full recapitulation of wing disc development *in vitro*.

Acknowledgements

We thank Florenci Serras for helpful guidance at the start of the project; J. Bischof, G. Hausmann and G. Reeves for providing critical comments on the manuscript; and S. Luschnig, C. Lehner, B. Handke, E. Hafen, G. Schwank, E. Brunner, W. Boll, D. Brunner and N. Dube for helpful feedback during the course of the project.

Funding

This work was supported by the NCCR Frontiers-in-Genetics doctoral school (S.R.); by an EMBO Long-term fellowship to J.Z.; and by the Swiss National Science Foundation, the Kanton of Zurich, the SystemsX.ch initiative within the framework of the WingX Project and the European Research Council under the European Community's Seventh Framework Programme.

Competing interests statement

The authors declare no competing financial interests.

Supplementary material

Supplementary material available online at
http://dev.biologists.org/lookup/suppl/doi:10.1242/dev.088872/-/DC1

References

Adler, P. N. and MacQueen, M. (1981). Partial coupling of the cell cycles of neighboring imaginal disc cells. *Exp. Cell Res.* **133**, 452-456.
Aegerter-Wilmsen, T., Smith, A. C., Christen, A. J., Aegerter, C. M., Hafen, E. and Basler, K. (2010). Exploring the effects of mechanical feedback on epithelial topology. *Development* **137**, 499-506.
Affolter, M. and Basler, K. (2007). The Decapentaplegic morphogen gradient: from pattern formation to growth regulation. *Nat. Rev. Genet.* **8**, 663-674.
Aldaz, S., Escudero, L. M. and Freeman, M. (2010). Live imaging of Drosophila imaginal disc development. *Proc. Natl. Acad. Sci. USA* **107**, 14217-14222.
Ashburner, M., Golic, K. G. and Hawley, R. S. (2005). *Drosophila: A Laboratory Handbook*. Cold Spring Harbor, NY: Cold Spring Harbor Laboratory Press.
Batista, F. R. X., Pereira, C. A., Mendonça, R. Z. and Moraes, A. M. (2008). Formulation of a protein-free medium based on IPL-41 for the sustained growth of Drosophila melanogaster S2 cells. *Cytotechnology* **57**, 11-22.
Belacortu, Y. and Paricio, N. (2011). Drosophila as a model of wound healing and tissue regeneration in vertebrates. *Dev. Dyn.* **240**, 2379-2404.
Bischof, J., Maeda, R. K., Hediger, M., Karch, F. and Basler, K. (2007). An optimized transgenesis system for Drosophila using germ-line-specific phiC31 integrases. *Proc. Natl. Acad. Sci. USA* **104**, 3312-3317.
Bovo, R., Galesi, A. L. L., Jorge, S. A. C., Piccoli, R. A. M., Moraes, A. M., Pereira, C. A. and Augusto, E. F. P. (2008). Kinetic response of a Drosophila melanogaster cell line to different medium formulations and culture conditions. *Cytotechnology* **57**, 23-35.
Bryant, P. J. and Fraser, S. E. (1988). Wound healing, cell communication, and DNA synthesis during imaginal disc regeneration in Drosophila. *Dev. Biol.* **127**, 197-208.
Cherbas, L., Willingham, A., Zhang, D., Yang, L., Zou, Y., Eads, B. D., Carlson, J. W., Landolin, J. M., Kapranov, P., Dumais, J. et al. (2011). The transcriptional diversity of 25 Drosophila cell lines. *Genome Res.* **21**, 301-314.
Classen, A.-K., Anderson, K. I., Marois, E. and Eaton, S. (2005). Hexagonal packing of Drosophila wing epithelial cells by the planar cell polarity pathway. *Dev. Cell* **9**, 805-817.
Crick, F. H. and Lawrence, P. A. (1975). Compartments and polyclones in insect development. *Science* **189**, 340-347.
Cullen, C. F. and Milner, M. J. (1991). Parameters of growth in primary cultures and cell lines established from Drosophila imaginal discs. *Tissue Cell* **23**, 29-39.
Currie, D. A., Milner, M. J. and Evans, C. W. (1988). The growth and differentiation in vitro of leg and wing imaginal disc cells from Drosophila melanogaster. *Development* **102**, 805-814.
De Celis, J. F. (2003). Pattern formation in the Drosophila wing: The development of the veins. *Bioessays* **25**, 443-451.

Eaton, S. (2003). Cell biology of planar polarity transmission in the Drosophila wing. *Mech. Dev.* **120**, 1257-1264.
Echalier, G. (1975). In vitro established lines of Drosophila cells and applications in physiological genetics. In *Invertebrate Tissue Culture: Applications in Medicine, Biology and Agriculture*, pp. 131-150. New York: Academic Press.
Echalier, G. (1997). *Drosophila Cells in Culture*. San Diego, CA: Academic Press.
Elliott, D. A. and Brand, A. H. (2008). The GAL4 system. In *Drosophila* (ed. C. Dahmann), pp. 79-95. Totowa, NJ: Humana Press.
Fain, M. J. and Stevens, B. (1982). Alterations in the cell cycle of Drosophila imaginal disc cells precede metamorphosis. *Dev. Biol.* **92**, 247-258.
Garcia-Bellido, A. and Merriam, J. R. (1971). Parameters of the wing imaginal disc development of Drosophila melanogaster. *Dev. Biol.* **24**, 61-87.
Gardiner, G. R. and Stockdale, H. (1975). Two tissue culture media for production of lepidopteran cells and nuclear polyhedrosis viruses. *J. Invert. Pathol.* **25**, 363-370.
Gibson, M. C., Patel, A. B., Nagpal, R. and Perrimon, N. (2006). The emergence of geometric order in proliferating metazoan epithelia. *Nature* **442**, 1038-1041.
Griffin, R., Sustar, A., Bonvin, M., Binari, R., del Valle Rodriguez, A., Hohl, A. M., Bateman, J. R., Villalta, C., Heffern, E., Grunwald, D. et al. (2009). The twin spot generator for differential Drosophila lineage analysis. *Nat. Methods* **6**, 600-602.
Huang, J., Zhou, W., Dong, W., Watson, A. M. and Hong, Y. (2009). Directed, efficient, and versatile modifications of the Drosophila genome by genomic engineering. *Proc. Natl. Acad. Sci. USA* **106**, 8284-8289.
Jeon, M. K., Lim, J.-B. and Lee, G. M. (2010). Development of a serum-free medium for in vitro expansion of human cytotoxic T lymphocytes using a statistical design. *BMC Biotechnol.* **10**, 70.
Jursnich, V. A., Fraser, S. E., Held, L. I., Jr, Ryerse, J. and Bryant, P. J. (1990). Defective gap-junctional communication associated with imaginal disc overgrowth and degeneration caused by mutations of the dco gene in Drosophila. *Dev. Biol.* **140**, 413-429.
Kawamura, K., Shibata, T., Saget, O., Peel, D. and Bryant, P. J. (1999). A new family of growth factors produced by the fat body and active on Drosophila imaginal disc cells. *Development* **126**, 211-219.
Kicheva, A., Pantazis, P., Bollenbach, T., Kalaidzidis, Y., Bittig, T., Jülicher, F. and González-Gaitán, M. (2007). Kinetics of morphogen gradient formation. *Science* **315**, 521-525.
Landsberg, K. P., Farhadifar, R., Ranft, J., Umetsu, D., Widmann, T. J., Bittig, T., Said, A., Jülicher, F. and Dahmann, C. (2009). Increased cell bond tension governs cell sorting at the Drosophila anteroposterior compartment boundary. *Curr. Biol.* **19**, 1950-1955.
Li, S. (2010). Identification of iron-loaded ferritin as an essential mitogen for cell proliferation and postembryonic development in Drosophila. *Cell Res.* **20**, 1148-1157.
Mandenius, C.-F. and Brundin, A. (2008). Bioprocess optimization using design-of-experiments methodology. *Biotechnol. Prog.* **24**, 1191-1203.
Mao, Y., Tournier, A. L., Bates, P. A., Gale, J. E., Tapon, N. and Thompson, B. J. (2011). Planar polarization of the atypical myosin Dachs orients cell divisions in Drosophila. *Genes Dev.* **25**, 131-136.
Milán, M., Campuzano, S. and García-Bellido, A. (1996). Cell cycling and patterned cell proliferation in the wing primordium of Drosophila. *Proc. Natl. Acad. Sci. USA* **93**, 640-645.
Neto-Silva, R. M., Wells, B. S. and Johnston, L. A. (2009). Mechanisms of growth and homeostasis in the Drosophila wing. *Annu. Rev. Cell Dev. Biol.* **25**, 197-220.
Neufeld, T. P., de la Cruz, A. F., Johnston, L. A. and Edgar, B. A. (1998). Coordination of growth and cell division in the Drosophila wing. *Cell* **93**, 1183-1193.
Ohsawa, S., Sugimura, K., Takino, K. and Igaki, T. (2012). Imaging cell competition in Drosophila imaginal discs. *Methods Enzymol.* **506**, 407-413.
Pearson, J., López-Onieva, L., Rojas-Ríos, P. and González-Reyes, A. (2009). Recent advances in Drosophila stem cell biology. *Int. J. Dev. Biol.* **53**, 1329-1339.
Robb, J. A. (1969). Maintenance of imaginal discs of Drosophila melanogaster in chemically defined media. *J. Cell Biol.* **41**, 876-885.
Scheffe, H. (1963). The simplex-centroid design for experiments with mixtures. *J. R. Stat. Soc. B Stat. Methodol.* **25**, 235-263.
Schneider, I (1964). Differentiation of larval Drosophila eye-antennal discs in vitro. *J. Exp. Zool.* **156**, 91-103.
Schwank, G., Tauriello, G., Yagi, R., Kranz, E., Koumoutsakos, P. and Basler, K. (2011). Antagonistic growth regulation by Dpp and Fat drives uniform cell proliferation. *Dev. Cell* **20**, 123-130.
Shields, G., Dübendorfer, A. and Sang, J. H. (1975). Differentiation in vitro of larval cell types from early embryonic cells of Drosophila melanogaster. *J. Embryol. Exp. Morphol.* **33**, 159-175.
Ui, K., Ueda, R. and Miyake, T. (1987). Cell lines from imaginal discs of Drosophila melanogaster. *In Vitro Cell. Dev. Biol.* **23**, 707-711.
Ursprung, H., Nöthiger, R., Fristrom, J. W. and Hadorn, E. (1972). *The Biology of Imaginal Disks.* Berlin, Germany: Springer.
Weiss, S. A., Smith, G. C., Kalter, S. S. and Vaughn, J. L. (1981). Improved method for the production of insect cell cultures in large volume. *In Vitro* **17**, 495-502.
Wyss, C. (1982). Ecdysterone, insulin and fly extract needed for the proliferation of normal Drosophila cells in defined medium. *Exp. Cell Res.* **139**, 297-307.
Yagi, R., Mayer, F. and Basler, K. (2010). Refined LexA transactivators and their use in combination with the Drosophila Gal4 system. *Proc. Natl. Acad. Sci. USA* **107**, 16166-16171.
Zurovec, M., Dolezal, T., Gazi, M., Pavlova, E. and Bryant, P. J. (2002). Adenosine deaminase-related growth factors stimulate cell proliferation in Drosophila by depleting extracellular adenosine. *Proc. Natl. Acad. Sci. USA* **99**, 4403-4408.

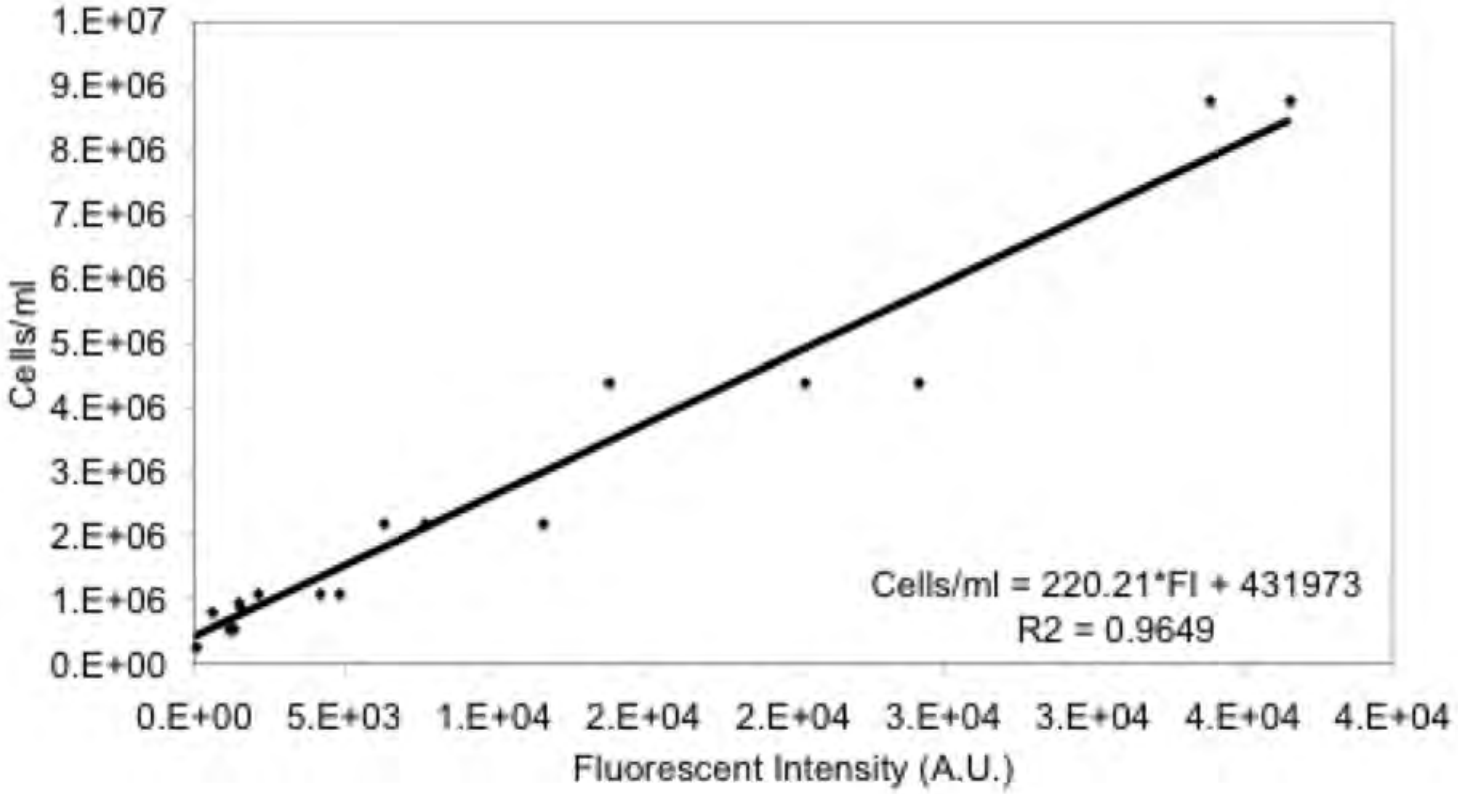

Fig. S1. Calibration curve demonstrating a linear relationship between CyQUANT Direct Proliferation dye and Cl.8 cell number.

Table S1: Composition of Cl. 8 Serum-containing medium (M3RM)

Components	Concentration	Source
Shield and Sang's M3 medium	94.5%	Sigma #S8398
Fetal bovine serum (FBS)	2%	Biochrom AG #50115
Bovine insulin	0.5% 0.05 mg/ml (0.125 IU/ml)	Sigma #I-6634, make 1 mg/ml stock in acidified water
Fly extract	2.5%	See Materials and methods for preparation.
Penicillin streptomycin (P/S)	0.5%	Gibco #15140 10,000 units/ml Penicillin, 10,000 µg/ml streptomycin

Table S2: Basal media tested in blending experiment

Var.	Basal medium	Notes	Xenogenic components	References
A	Shields and Sang's M3	Basal medium for SCM.	1 g/l TC Yeastolate	(Shields et al., 1975)
B	Schneider's medium	S2 cells	2 g/l TC Yeastolate	(Schneider, 1964)
C	D-22	Kc cells		(Echalier, 1975)
D	IPL-41	Lepidopteran, useful basis for serum free media	None	(Weiss et al., 1981)
E	TC-100	Variant of Grace's medium	Tryptose broth	(Gardiner and Stockdale, 1975)
F	Sf-900 II SFM	Protein free medium for Sf 9	Proprietary formula.	Invitrogen

Table S3: Experimental design for blending experiment with response values

Std	Run	Block	Type	A	B	C	D	E	F	Response	
				M3	Sch	D22	IPL41	TC100	Sf900II	Avg	St. Dev.
1	87	4	Vertex	1	0	0	0	0	0	11722	813
2	26	2	Vertex	0	1	0	0	0	0	10949	2871
3	37	2	Vertex	0	0	1	0	0	0	486	449
4	71	3	Vertex	0	0	0	1	0	0	10054	838
5	81	4	Vertex	0	0	0	0	1	0	7579	493
6	22	1	Vertex	0	0	0	0	0	1	0	22
7	23	1	CentEdge	0.5	0.5	0	0	0	0	8542	976
8	11	1	CentEdge	0.5	0	0.5	0	0	0	6887	2373
9	86	4	CentEdge	0.5	0	0	0.5	0	0	8001	204
10	29	2	CentEdge	0.5	0	0	0	0.5	0	7156	2941
11	41	2	CentEdge	0.5	0	0	0	0	0.5	11477	801
12	27	2	CentEdge	0	0.5	0.5	0	0	0	1114	216
13	21	1	CentEdge	0	0.5	0	0.5	0	0	9264	398
14	14	1	CentEdge	0	0.5	0	0	0.5	0	8598	650
15	74	4	CentEdge	0	0.5	0	0	0	0.5	15930	1108
16	56	3	CentEdge	0	0	0.5	0.5	0	0	4536	703
17	64	3	CentEdge	0	0	0.5	0	0.5	0	6993	699
18	33	2	CentEdge	0	0	0.5	0	0	0.5	39	314
19	20	1	CentEdge	0	0	0	0.5	0.5	0	4987	579
20	90	4	CentEdge	0	0	0	0.5	0	0.5	11031	516
21	52	3	CentEdge	0	0	0	0	0.5	0.5	7388	2605
22	82	4	TripBlend	0.33	0.33	0.33	0	0	0	11447	700
23	54	3	TripBlend	0.33	0.33	0	0.33	0	0	9022	768
24	53	3	TripBlend	0.33	0.33	0	0	0.33	0	8934	1271
25	63	3	TripBlend	0.33	0.33	0	0	0	0.33	16991	630
26	36	2	TripBlend	0.33	0	0.33	0.33	0	0	6289	1484
27	34	2	TripBlend	0.33	0	0.33	0	0.33	0	5937	294
28	79	4	TripBlend	0.33	0	0.33	0	0	0.33	10352	2006
29	57	3	TripBlend	0.33	0	0	0.33	0.33	0	10503	781
30	13	1	TripBlend	0.33	0	0	0.33	0	0.33	5294	719
31	78	4	TripBlend	0.33	0	0	0	0.33	0.33	12929	627
32	93	4	TripBlend	0	0.33	0.33	0.33	0	0	12391	312
33	45	2	TripBlend	0	0.33	0.33	0	0.33	0	11876	1059

34	3	1	TripBlend	0	0.33	0.33	0	0	0.33	5053	800
35	43	2	TripBlend	0	0.33	0	0.33	0.33	0	12309	791
36	61	3	TripBlend	0	0.33	0	0.33	0	0.33	19618	655
37	31	2	TripBlend	0	0.33	0	0	0.33	0.33	6225	822
38	40	2	TripBlend	0	0	0.33	0.33	0.33	0	3839	307
39	91	4	TripBlend	0	0	0.33	0.33	0	0.33	8604	544
40	84	4	TripBlend	0	0	0.33	0	0.33	0.33	10615	583
41	6	1	TripBlend	0	0	0	0.33	0.33	0.33	4357	272
42	25	2	4 Blend	0.25	0.25	0.25	0.25	0	0	7121	907
43	88	4	4 Blend	0.25	0.25	0.25	0	0.25	0	13260	680
44	4	1	4 Blend	0.25	0.25	0.25	0	0	0.25	8846	944
45	30	2	4 Blend	0.25	0.25	0	0.25	0.25	0	10615	607
46	47	2	4 Blend	0.25	0.25	0	0.25	0	0.25	11104	1976
47	96	4	4 Blend	0.25	0.25	0	0	0.25	0.25	15104	1423
48	55	3	4 Blend	0.25	0	0.25	0.25	0.25	0	6425	920
49	42	2	4 Blend	0.25	0	0.25	0.25	0	0.25	10349	2079
50	8	1	4 Blend	0.25	0	0.25	0	0.25	0.25	5248	534
51	72	3	4 Blend	0.25	0	0	0.25	0.25	0.25	11789	396
52	89	4	4 Blend	0	0.25	0.25	0.25	0.25	0	10790	262
53	19	1	4 Blend	0	0.25	0.25	0.25	0	0.25	6059	1308
54	73	4	4 Blend	0	0.25	0.25	0	0.25	0.25	13416	1256
55	66	3	4 Blend	0	0.25	0	0.25	0.25	0.25	14597	149
56	35	2	4 Blend	0	0	0.25	0.25	0.25	0.25	2511	244
57	85	4	5 Blend	0.2	0.2	0.2	0.2	0.2	0	13738	832
58	68	3	5 Blend	0.2	0.2	0.2	0.2	0	0.2	14927	680
59	75	4	5 Blend	0.2	0.2	0.2	0	0.2	0.2	14631	707
60	77	4	5 Blend	0.2	0.2	0	0.2	0.2	0.2	15628	336
61	12	1	5 Blend	0.2	0	0.2	0.2	0.2	0.2	5862	1269
62	49	3	5 Blend	0	0.2	0.2	0.2	0.2	0.2	4249	7516
63	18	1	Center	0.17	0.17	0.17	0.17	0.17	0.17	7375	866
64	32	2	AxialCB	0.58	0.08	0.08	0.08	0.08	0.08	8321	2071
65	9	1	AxialCB	0.08	0.58	0.08	0.08	0.08	0.08	11326	1942
66	62	3	AxialCB	0.08	0.08	0.58	0.08	0.08	0.08	12915	189
67	83	4	AxialCB	0.08	0.08	0.08	0.58	0.08	0.08	14610	123
68	15	1	AxialCB	0.08	0.08	0.08	0.08	0.58	0.08	5817	346
69	2	1	AxialCB	0.08	0.08	0.08	0.08	0.08	0.58	3902	450
70	10	1	Vertex	1	0	0	0	0	0	9947	1151
71	58	3	Vertex	0	1	0	0	0	0	25443	1563

72	94	4	Vertex	0	0	1	0	0	0	1333	624
73	5	1	Vertex	0	0	0	1	0	0	5144	916
74	48	2	Vertex	0	0	0	0	1	0	6041	181
75	70	3	Vertex	0	0	0	0	0	1	2076	42
76	39	2	CentEdge	0.5	0.5	0	0	0	0	10122	1419
77	7	1	CentEdge	0	0	0.5	0.5	0	0	2992	1234
78	44	2	CentEdge	0	0	0	0	0.5	0.5	8558	2248
79	65	3	CentEdge	0.5	0	0.5	0	0	0	10605	66
80	76	4	CentEdge	0	0.5	0	0.5	0	0	17320	1271
81	16	1	CentEdge	0.5	0	0	0	0.5	0	5895	632
82	38	2	CentEdge	0	0.5	0	0	0	0.5	6546	938
83	67	3	CentEdge	0	0	0.5	0	0	0.5	6172	1315
84	92	4	CentEdge	0	0	0	0.5	0.5	0	9248	1059
85	1	1	CentEdge	0.5	0	0	0.5	0	0	9132	1454
86	50	3	CentEdge	0	0.5	0.5	0	0	0	6148	1133
87	51	3	CentEdge	0.5	0	0	0	0	0.5	3733	226
88	59	3	CentEdge	0	0.5	0	0	0.5	0	14925	379
89	24	1	CentEdge	0	0	0.5	0	0.5	0	1565	308
90	46	2	CentEdge	0	0	0	0.5	0	0.5	10511	2139
91	60	3	Vertex	1	0	0	0	0	0	15228	289
92	95	4	Vertex	0	1	0	0	0	0	17518	955
93	17	1	Vertex	0	0	1	0	0	0	128	118
94	28	2	Vertex	0	0	0	1	0	0	13022	1725
95	69	3	Vertex	0	0	0	0	1	0	8907	152
96	80	4	Vertex	0	0	0	0	0	1	1141	58

Table S4. ANOVA summary for blending experiment (Partial Sum of Squares, Type III)

Source	Sum of squares	df	Mean Square	F value	*P*-value
Block	16440.7	3	5480.3		
Model	47894.9	12	3991.2	19.5	< 0.0001
Linear Mixture	34447.3	5	6889.5	33.7	< 0.0001
AC	2458.3	1	2458.3	12.0	0.0009
AF	3633.5	1	3633.5	17.8	< 0.0001
BF	2059.0	1	2059.0	10.1	0.0022
CE	625.5	1	625.5	3.1	0.0842
CF	1126.2	1	1126.2	5.5	0.0215
DF	2751.9	1	2751.9	13.5	0.0004
EF	1748.9	1	1748.9	8.6	0.0045
Residual	16162.2	79	204.6		

Table S5. Coefficients (real components) for blending experiment model

Coefficient	Standard			95% CI	95% CI
Component	Estimate	df	Error	Low	High
Plate1	-16.5	3.0			
Plate2	-9.1				
Plate3	11.1				
Plate4	14.5				
A-M3	99.3	1.0	6.5	86.4	112.2
B-Sch	127.3	1.0	6.0	115.3	139.2
C-D22	26.3	1.0	7.0	12.4	40.2
D-IPL-41	98.0	1.0	6.0	86.1	109.9
E-TC-100	81.3	1.0	6.5	68.4	94.2
F-Sf900 II	23.4	1.0	8.1	7.4	39.4
AC	132.6	1.0	38.3	56.5	208.8
AF	187.5	1.0	44.5	99.0	276.1
BF	121.6	1.0	38.3	45.3	197.8
CE	66.8	1.0	38.2	-9.2	142.7
CF	90.0	1.0	38.4	13.7	166.4
DF	140.7	1.0	38.4	64.3	217.1

Table S6. Factor levels for RSM

Factors	Levels		
	-1	0	1
Insulin	0	.05 mg/ml	0.1 mg/ml
FBS	0	2%	4%
FEX	0	2.50%	5%
Basal medium	M3		Schneider's

Table S7. Experimental design for RSM

Std	Run	Insulin	FBS	FEX	Basal	Fluor. Int. (A.U.)
Block 1						
32	1	0	0	0	{ 1 }	32051
27	2	-1	1	1	{ 1 }	17010
12	3	0	0	0	{ -1 }	15821
1	4	-1	-1	-1	{ -1 }	1088
30	5	0	0	0	{ 1 }	31164
4	6	1	1	-1	{ -1 }	2009
2	7	1	-1	-1	{ -1 }	957
31	8	0	0	0	{ 1 }	28191
26	9	1	-1	1	{ 1 }	31531
6	10	1	-1	1	{ -1 }	20957
9	11	0	0	0	{ -1 }	15026
10	12	0	0	0	{ -1 }	15050
5	13	-1	-1	1	{ -1 }	16958
21	14	-1	-1	-1	{ 1 }	*
11	15	0	0	0	{ -1 }	13540
8	16	1	1	1	{ -1 }	27044
23	17	-1	1	-1	{ 1 }	*
22	18	1	-1	-1	{ 1 }	*
29	19	0	0	0	{ 1 }	25798
Block 2						
14	20	1	0	0	{ -1 }	13125
18	21	0	0	1	{ -1 }	31012
35	22	0	-1	0	{ 1 }	27639
20	23	0	0	0	{ -1 }	14564
16	24	0	1	0	{ -1 }	20290
19	25	0	0	0	{ -1 }	14999
15	26	0	-1	0	{ -1 }	12131
33	27	-1	0	0	{ 1 }	14261
36	28	0	1	0	{ 1 }	25268
39	29	0	0	0	{ 1 }	28297
38	30	0	0	1	{ 1 }	41343
37	31	0	0	-1	{ 1 }	3434
34	32	1	0	0	{ 1 }	30488
40	33	0	0	0	{ 1 }	23443
17	34	0	0	-1	{ -1 }	224
13	35	-1	0	0	{ -1 }	12557
24	36	1	1	-1	{ 1 }	3124
7	37	-1	1	1	{ -1 }	16788

25	38	-1	-1	1	{ 1 }	17075
3	39	-1	1	-1	{ -1 }	2358
28	40	1	1	1	{ 1 }	17945

Table S8. ANOVA summary for RSM experiment

Source	Sum of Squares	df	Mean square	F value	*P* value
Block	44.92	2	22.46		
Model	123996.65	20	6199.83	71.98	< 0.0001
A-Insulin	33.84	1	33.84	0.39	0.53
B-FBS	1274.21	1	1274.21	14.79	0.00
C-FEX	3801.30	1	3801.30	44.13	< 0.0001
D-Basal med.	12858.14	1	12858.14	149.28	< 0.0001
AB	33.51	1	33.51	0.39	0.54
AC	179.07	1	179.07	2.08	0.16
AD	547.53	1	547.53	6.36	0.02
BC	0.00	1	0.00	0.00	1.00
BD	1259.38	1	1259.38	14.62	0.00
CD	1329.01	1	1329.01	15.43	0.00
A^2	1087.07	1	1087.07	12.62	0.00
B^2	0.23	1	0.23	0.00	0.96
C^2	6357.79	1	6357.79	73.81	< 0.0001
A^{2B}	346.97	1	346.97	4.03	0.05
A^{2C}	365.89	1	365.89	4.25	0.05
A^{2D}	609.68	1	609.68	7.08	0.01
B^{2C}	617.50	1	617.50	7.17	0.01
A^3	306.94	1	306.94	3.56	0.07
B^3	482.77	1	482.77	5.60	0.02
C^3	1623.14	1	1623.14	18.84	0.00
Residual	3273.17	38	86.14		
Lack of Fit	2219.66	21	105.70	1.71	0.13
Pure Error	1053.51	17	61.97		
Cor Total	127314.74	60			

Table S9. Coefficients (coded) for RSM experiment

Factor	Coefficient estimate	df	Standard error	95% CI low	95% CI high
Intercept	150	1	2	146	154
Block 1	-2	2			
Block 2	-9				
Block 3	11				
A-Insulin	-4	1	7	-18	9
B-FBS	25	1	6	12	37
C-FEX	42	1	6	29	55
D-Basal	22	1	2	18	25
AB	-2	1	2	-6	3
AC	3	1	2	-1	8
AD	5	1	2	1	9
BC	0	1	3	-5	5
BD	-9	1	2	-13	-4
CD	-9	1	2	-13	-4
A^2	-14	1	4	-22	-6
B^2	0	1	4	-8	8
C^2	-31	1	4	-38	-23
A^2B	-10	1	5	-20	0
A^2C	-13	1	6	-26	0
A^2D	-9	1	3	-15	-2
B^2C	-19	1	7	-33	-5
A^3	14	1	7	-1	29
B^3	-17	1	7	-32	-3
C^3	33	1	8	17	48

Appendix S1

Additional notes on data analysis

Blending experiment data analysis

A square root transformation was applied to the data (as suggested from a Box-Cox plot). Regression analysis resulted in a reduced quadratic Scheffe model (forward regression, alpha = 0.1). The reduced model gives an R^2 of 0.74, with an adjusted R^2 of 0.70 and a predictive R^2 of 0.61.

Additional notes on the execution of the RSM experiment

Initially, a face-centered composite design was chosen for the first two blocks to fit a quadratic model to the response data, but this was insufficient to provide a significant model with an insignificant lack of fit. One explanation for the insufficiency of the experimental design could be the cubic nature of the response.

The design was subsequently augmented with a third block added. Experimental design points using Design-Expert® were chosen to make the design IV-optimal. The final design included a total of 64 runs distributed over 3 blocks. Supp. Table 8-9 present the experimental design in coded form as well as the response data. In the first block, several readings resulted in negative numbers due to abnormally high background fluorescent readings. These data points were excluded from analysis as the cause of the aberrant readings could not be identified, but inclusion did not seem to affect the main conclusions..

Data analysis for the RSM Experiment

A square-root transformation was again applied to the data (counting data). The ANOVA analysis is presented in Table 6. Regression was performed with backward elimination ($\alpha = 0.1$) to provide a reduced cubic model with an R^2 value of 0.98 (Adjusted-R^2 = 0.97, Predictive-R^2=0.94). The lack of fit was deemed non-significant with a p-value of 0.13. Table 7 provides estimates of the coefficients in terms of coded factors.